	PLAN	**Doc. no.** : SRON-XMS-PL-2009-004 **Issue** : 1 **Date** : 16 June 2010 **Cat** : **Page** : 1 of 1
IXO		

Title : **IXO-XMS LVSID Anti-coincidence Detector**

Prepared by : F. Scott Porter/GSFC
Caroline Kilbourne/GSFC

Date : 16 June 2010

Checked by :

Date :

PA agreed by :

Date :

Authorised by :

Date :

Distribution

Document Change Record

Issue	Date	Changed Section	Description of Change

Table of contents

In order to update the table, click right on a table item and select "Update Field" followed by "Update entire table". Delete this text of course.

Abbreviations and acronyms

Item	Meaning

Applicable Documents

[AD#]	Doc. Reference	Issue	Title
[AD1]			
[AD2]			
[AD3]			
[AD4]			
[AD5]			
[AD6]			

Reference Documents

[RD#]	Doc. Reference	Issue	Title
[RD1]			
[RD2]			
[RD3]			
[RD4]			
[RD5]			
[RD6]			

I. Introduction

This document describes a high-TRL backup implementation of the anti-coincidence detector for the IXO/XMS instrument. The backup detector, hereafter referred to as the low-voltage silicon ionization detector (LVSID), has been successfully flown on Astro-E2 (Suzaku)/XRS and is currently being implemented, without significant changes, on the Astro-H/SXS instrument. The LVSID anti-coincidence detector on Astro-E2/XRS operated successfully for almost 2 years, and was not affected by the loss of liquid helium in that instrument. The LVSID continues to operate after almost 5 years on-orbit (LEO, 550 km) but with slightly increased noise following the expected depletion of solid Neon after 22 months. The noise of the device is increased after the loss of sNe due to thermally induced bias and readout noise. No radiation damage, or off-nominal affects have been observed with the LVSID on-orbit during the Astro-E2/XRS program. A detector die from the same fabrication run will be used on the Astro-H/SXS mission. The LVSID technology and cryogenic JFET readout system is thus TRL 9. The technology is described in detail in section 2.

The IXO/XMS "backup-up" anti-coincidence detector is a small array of LVSID detectors that are almost identical to those employed for Astro-E2/XRS as described in this document. The readout system is identical and, in-fact would use the same design as the Astro-E2/XRS JFET amplifier module (19 channels) essentially without changes except for its mechanical mount. The changes required for the IXO/XMS LVSID array are limited to the mounting of the LVSID detectors, and the mechanical mounting of the JFET amplifier sub-assembly. There is no technical development needed for the IXO/XMS implementation and the technology is ready for detailed design-work leading to PDR. The TRL level is thus at least 6, and possibly higher. Characteristics of an IXO/XMS LVSID anti-co detector are given in Table 1 and described in detail in section 3.

II. Description of the XMS LVSID anti-co

1 Requirements

Requirements for the "back-up" anti-coincidence option are the same as the "primary" option as far as threshold energy, geometric rejection, timing, etc…

Table 1. LVSID detector characteristics based on the demonstrated performance of the Astro-E2/XRS anti-co detector on orbit.

Characteristic	**Best estimate**
Detector size	39.4 mm
Detector layers	2
Segments (die)/layer	9
Segment size	1.3 x 1.3 cm x 0.5 mm
Rise time	10 us
Fall time	130 us (design parameter)
Threshold	10-20 keV (design parameter)
Operating temperature	0.05-100 K
JFET channels	18
JFET temperature	130K
JFET module heat sink T	0.5-5K
JFET heat load 50 mK	0.05 uW (wiring)

JFET heat load 4K	25 uW
JFET heat load 15-20K	6 mW

2 Description of principle

2.1 Anti-coicidence detector for the Astro-E2 (Suzaku)/XRS instrument

The Astro-E2 (Suzaku) X-ray Spectrometer (XRS) is the logical predecessor to the IXO/XMS instrument. The XRS consisted of 32 cryogenic x-ray detectors operated at 60 mK and cooled by an adiabatic demagnetization refrigerator. The XRS detector system used an LVSID anti-coincidence detector placed directly behind the detector array to veto events in the main-array due to minimum ionizing particles. A conceptual drawing of this arrangement is shown in Figure 1. The XRS instrument operated for about 6 weeks on orbit before a flaw in the accommodation of the experiment caused the pre-mature loss of LHe and the end of the science capability of the instrument. The LVSID anti-coincidence detector, however, continues to operate after nearly 5 years on orbit (launch July 10, 2005), with no sign of degradation in low-earth orbit (550 km) although the noise of the bias and readout has increased slightly after the solid Neon cryogen was exhausted after 22 months on orbit. The Astro-E2 LVSID anti-coincidence detector forms the basis of the backup anti-coincidence detector for the IXO/XMS instrument and is described in briefly in this section. For a more complete description of the XRS instrument see Kelley et al., 2007. In addition, an identical anti-co detector will fly as part of the SXS cryogenic x-ray spectrometer on the Astro-H mission in 2014. This is discussed in section 2.2.

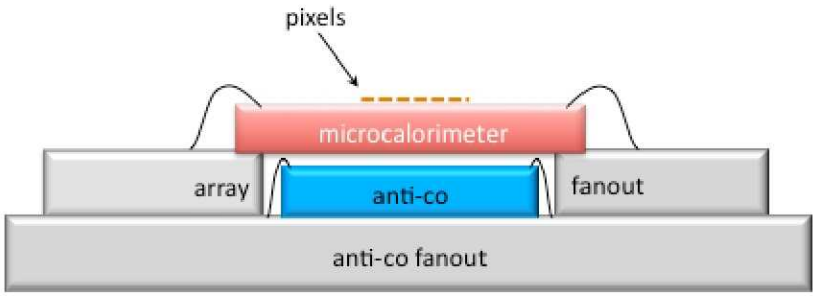

Figure 1. Schematic arrangement of the Astro-E2/XRS microcalorimeter detector array and the LVSID anti-coincidence detector. The Astro-H/SXS implementation is identical

Because a fraction of cosmic rays that traverse the calorimeter pixels will leave behind energy comparable to photons in the XRS spectral bandwidth, an anticoincidence detector was implemented both to reject cosmic ray events and to be an independent monitor of the particle environment. We chose to employ a silicon ionization detector rather than another calorimeter in order to provide a faster signal with temperature invariant gain that could provide diagnostic information in the event of signal saturation on the calorimeter array. The XRS anticoincidence detector was designed to operate at the calorimeter heat sink temperature (60mK) at low (< 9 V) bias so that it could be placed directly behind the calorimeter array. The sensor itself is a very simple design. The chip consists of 1 cm^2 × 0.5 mm of high purity silicon (nominally 13–21 kΩ cm at room temperature). One surface is degenerately doped with phosphorus (n+) while the other is degenerately doped with boron (p+), and both sides are metalized with aluminum. Thus it is configured as a p-i-n diode and is operated with the standard reverse-bias relative to that configuration. The

device should not be considered a diode at an operating temperature of 60 mK, however, because the carriers in the central intrinsic region are completely frozen out and the detector is simply an insulator between metallic contacts. Thus the device is more properly a low voltage silicon ionization detector (LVSID). Biases up to 24 V were investigated and no change in gain was seen for biases above 2 V. The XRS anticoincidence detector was biased at 6 V using the circuit shown in figure 2. We patterned the contacts so that their edges were 0.15 mm from the physical edge of the chip (shown in figure 3), which was itself defined by DRIE. The corners of both the physical and the electrical perimeter were rounded. Thus we eliminated uncontrolled field-concentrating features and a possible breakdown path along dicing-induced surface states at the edge. Figure 4 shows an LVSID pulse due to a single 60 keV gamma-ray giving a pulse rise time of 12 us and a pulse fall time of 260 us, limited by the LVSID capacitance and parasitic capacitance in the redundant readout circuit. The readout capacitance is about 1.3x the LVSID capacitance. A single string readout circuit, as proposed for IXO/XMS, would have produced a pulse 30% faster and with 30% more signal.

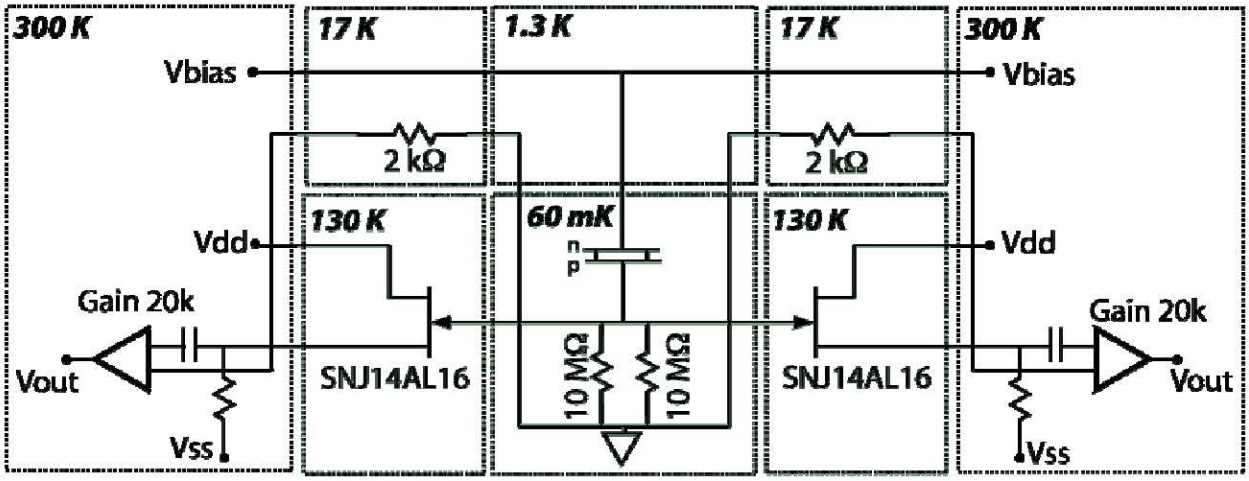

Figure 2. Readout circuit for the Astro-E2/XRS LVSID anti-co detector. Since there is only a single anti-co detector, it is designed with redundant readout nodes. The Astro-H/SXS anti-co detector and readout is identical except for slightly different thermal staging of the FETs (28K) and the LVSID detector (50mK), and a smaller bias resistor to increase the speed.

For Astro-E2, the pulse spectrum of the anticoincidence detector is not accumulated. Rather, the signal is compared to a commandable threshold, and if the signal exceeds that threshold during a time window associated with each calorimeter pulse, then the calorimeter signal is flagged. The energy equivalent of the 1σ value of the voltage noise was 1.6 keV. The default threshold was 16 keV, which was well below the 195 keV deposited by a minimum ionizing particle traversing the anticoincidence detector (0.5 mm of Si).

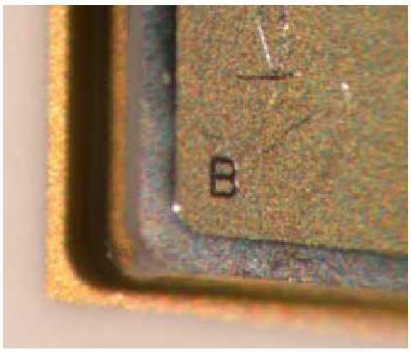

Figure 3. Closeup of a corner of the 1 cm^2 x 0.5 mm thick XRS LVSID detector showing the 0.15 mm pullback of the contacts from the edge of the die. This is done to minimize the chance of charge breakdown at the edges of the device. The "B" in the corner denotes the side doped with Boron. A larger view of the device is in figure 6.

The calorimeter array was mounted on an alumina board that was placed directly on top of the anticoincidence detector board, with the anticoincidence detector itself fitting in a hole in the array board as shown in figure 1. The top surface of the particle detector sits 0.63 mm below the plane of the calorimeter pixels. Considering an isotropic flux of minimum-ionizing particles, 98% of those impacting the calorimeter array will pass through the anticoincidence detector. Those that miss the anticoincidence detector tend to have longer path lengths in the HgTe absorbers, enhancing their rejection based on their being out of the observational band. Using a GEANT2 model, we determined that less than 0.1% of all incident minimum ionizing particles will deposit energy in the calorimeter of less than 10 keV without triggering the anticoincidence detector (Saab et al. 2004). An attempt was also made to model the unrejected background from secondary particles. The resulting prediction, though larger than that calculated for direct interaction of primary cosmic rays only, was less than that expected from scaling from the ASCA SIS background (Gendreau 1995), which was itself less than what was observed in orbit (see 2.1.1). The underestimate is presumed due to the low-fidelity model used to describe the surrounding structure and from the failure to include all the relevant interactions in the simulation.

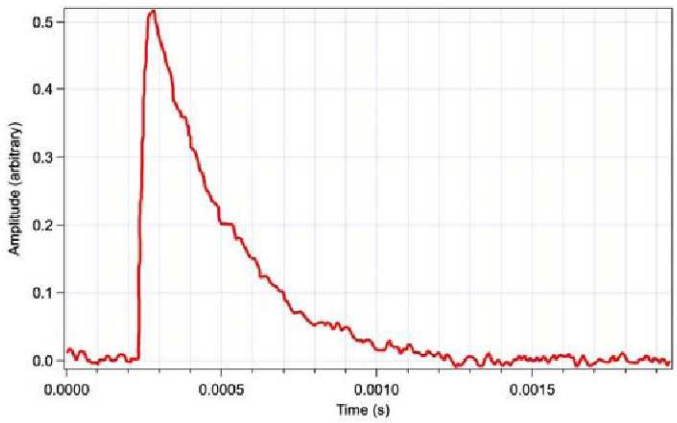

Figure 4. Single 60 keV gamma ray measured with the XRS LVSID anti-coincidence detector. The pulse has a risetime of 12 us and a falltime of 260 us, limited by the LVSID capacitance and the stray capacitance in the redundant readout circuit as shown in figure 2.

2.1.1 On orbit performance of the Astro-E2/XRS anti-co

The anticoincidence detector was operational for two weeks prior to the first ADR cycle, providing a preview of the particle background and allowing experimentation with the anticoincidence threshold. Outside of the SAA, the measured rate ranged from 0.3 to 2 c s^{-1} in the detector (1 cm^2 area), and the rate was inversely correlated with the geomagnetic cut-off rigidity, as expected. The threshold experiments showed that roughly half of the events deposit more than 430 keV (the highest setting for the threshold). Thus the spectrum is much harder than expected for minimum ionizing particles alone, for which 80% of the events would have been below 430 keV. A preliminary attempt to simulate secondary particles using a GEANT model made the spectrum somewhat harder, but still did not match the data.

We evaluated the XRS instrument background with the gate valve closed in a continuous 37103 s interval between crossings of the SAA. The science array experienced 850366 valid triggers between 0.1 and 12keV in the 30 pixels. To identify pulses from frame events (thermal crosstalk from particle events in the silicon frame of the detector array), we used a simple algorithm developed from analysis of the ground background data; this algorithm uses a single correlation interval of 0.5ms and rejects groups of correlated events of as few as two events. The calibration pixel is included in the screening for correlated events because electrons that escape upon X-ray absorption in the calibration pixel can be detected on the main array (Kilbourne et al. 2006). More sophisticated screening that would, among other tests, consider the energy of the calibration pixel events and use a shorter coincidence window for pairs would minimize dead time without sacrificing the effectiveness of the screening, but this software was not developed. After removing events within 0.5 ms of another event and events with the anticoincidence flag, we had 207 events remaining. This corresponds to a rate of 5×10^{-2} c s^{-1} cm^{-2} (0.1–12 keV). The spectrum of the background events (excluding low-resolution events, which removes 14 events) is shown in figure 5; there are no lines apparent with these statistics. The average rate in the anticoincidence detector during that time interval was 0.9 c s^{-1} cm^{-2} . If this rate were generated by minimum ionizing particles, then the background rate in the calorimeter after applying the anticoincidence veto would be 9×10^{-4} c s^{-1} cm^{-2}, so the measured residual background is dominated by secondary particles, as expected. The rate of frame events (for which one group of correlated calorimeter pulses is considered a single event) also works out to 0.9 c s^{-1} cm^{-2} of frame area, though the different effective thresholds and the shielding of the anticoincidence detector by the calorimeter chip make it unlikely that the two rates refer precisely to the same population of events.

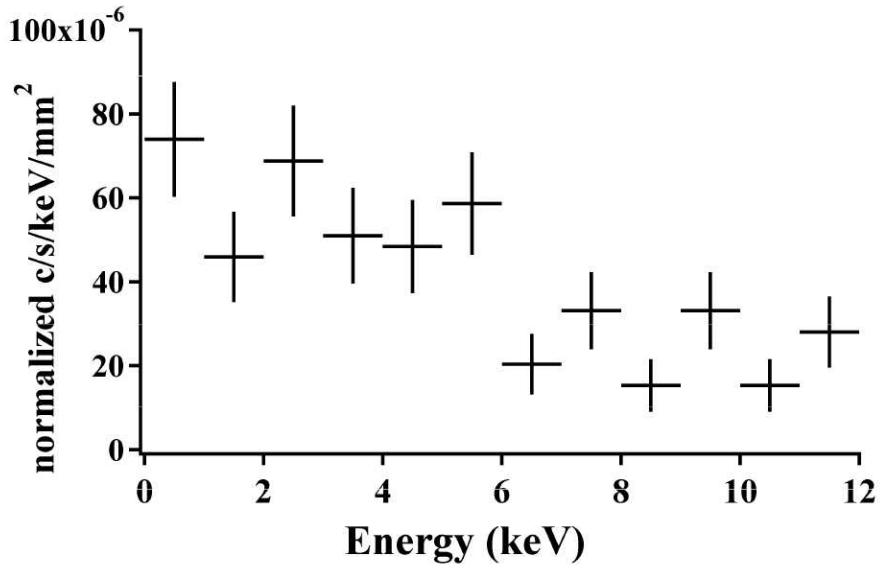

Figure 5. XRS residual background spectrum using the main detector array correlated with the LVSID anti-coincidence detector on-orbit.

Another view of the particle environment is provided by counting all events that involve direct deposition of energy in a calorimeter absorber and the anticoincidence detector. Because there is a narrow acceptance angle for incident particles to hit an absorber and the anticoincidence detector but not the calorimeter frame, we must identify the frame events that also contain a pulse from a direct absorber hit. This is easily done by taking the ratio of the biggest pulse to the second-biggest pulse in a frame event cluster. The pulses of most frame events are similar in energy, but there is a distinct population for which the biggest pulse is greater than six times the height of the next biggest pulse. Tallying the veto-flagged events among these pulses and the isolated pulses (making no energy cuts) results in a rate of 0.55 c s^{-1} cm^{-2}. Even this rate is likely to be dominated by high-energy secondary particles because the range in cut-off rigidity sampled by the Suzaku orbit should have reduced the 1 c s^{-1} cm^{-2} primary cosmic ray rate (in low Earth orbit in a flat detector at solar minimum) by more than a factor of five. More sophisticated GEANT models are needed to understand the nature of the secondary particles.

2.2 Anti-coincidence detector for Astro-H/SXS

The Astro-H Soft X-ray Spectrometer (SXS) instrument is similar to the XRS instrument but with a redundant cryogenic system, not limited by cryogen lifetime. The x-ray microcalorimeter array is similar to that used in XRS but with larger, higher performance x-ray absorbers covering a larger focal plane area. The anti-coincidence detector is identical to that used in the XRS instrument and was in-fact produced in the same fabrication run. The mounting board is slightly redesigned for SXS to accommodate a different focal plane mount and electrical pathways in the focal plane assembly. The SXS mechanical model anti-co detector is shown in Figure 6. Note that the mechanical model is a flight anti-co detector and anti-co mounting board but was used for bond shear testing.

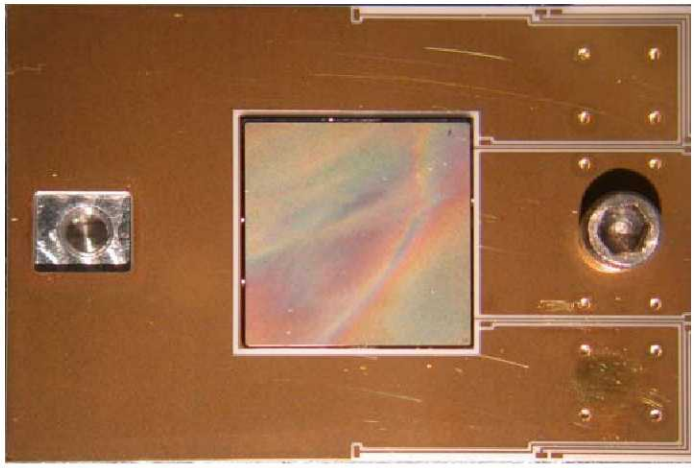

Figure 6. Mechanical model of the Astro-H/SXS LVSID anti-coincidence (center) attached to its gold plated high purity alumina mounting board. Note that the LVSID and mounting board are working flight parts assembled for bond shear testing. The LVSID die is 1.0 x 1.0 cm x 0.5 mm thick.

The only significant difference between the anti-co detectors on Astro-E2/XRS and Astro-H/SXS is in the pulse processing algorithm and in the bias resistor. The bias resistors for SXS speed up the fall time of the anti-co by about a factor of two compared to the pulse shown in figure 4, i.e. about 130 us fall time. On Astro-E2 the anti-co signal was compared to a defined threshold which was used to trigger a predefined veto window. On Astro-H the anti-co pulses are digitized and processed using the same digital pulse processing algorithms as the main detector array. This allows the Astro-H/SXS anti-co to be used for spectroscopy and for more advanced veto windows than that on Astro-E2. Similar anti-co processing is planned for IXO/XMS.

3 Design concept for an LVSID anti-co detector for IXO/XMS

The "backup" anti-co detector for the IXO/XMS instrument is a simple array of Astro/E2 (and Astro-H) LVSID detectors arranged in a grid under the main detector in the same configuration as used for Astro-E2 (Figure 1). We will use an array of 9 1.3 x 1.3 cm x 0.5 mm thick LVSID detectors with a 0.5 mm gap between them. The gap is formed from a 0.15 mm pull back of the implanted and metalized region of each device to eliminate any chance of charge breakdown at the edges (see Figure 3) and a 0.2 mm physical gap between devices. The device edges are lithographically defined and fabricated using deep reactive ion etching (DRIE) making extremely high precision edges. These devices are dimensionally almost identical to those used for Astro-E2 and Astro-H with about 70% larger surface area/device and thus about 70% higher capacitance. However, the total capacitance of the IXO LVSID and a single readout node (49 pf) is almost identical to the capacitance of the Astro-E2 LVSID and double readout node (48 pF) so the time constants will be the same. For IXO/XMS we will also use a smaller bias resistors as in the Astro-H/SXS (see section 2.2) which speeds up the falltime by a factor of two to about 130 us. The expected characteristics of the IXO/XMS LVSID array are given in Table 1.

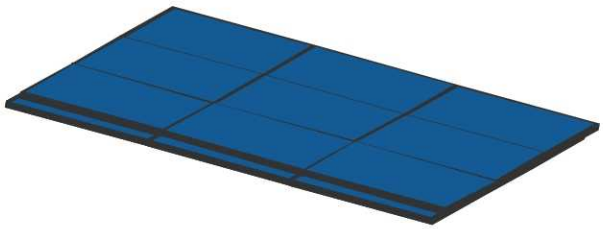

Figure 7. Design concept for the "backup" IXO/XMS anti-coincidence detector based on a simple array of Astro-E2-like LVSID detectors. The individual detectors are 1.3 x 1.3 cm x 0.5 mm thick. They are arranged in two layers of 3x3 devices for geometric coverage.

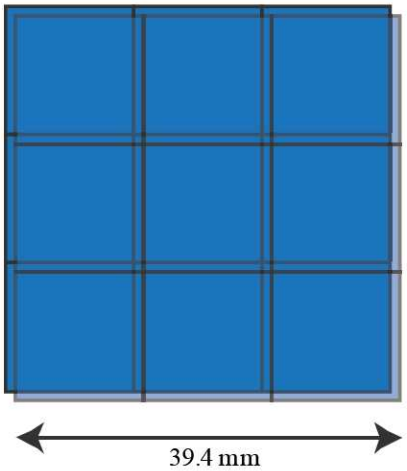

Figure 8. The two layers of LVSID detectors are offset by 2mm in x and y as shown in order to minimize the geometric area of the 0.5 mm gaps between the LVSID "pixels". The residual 8 intersection points on the interior of the area are 0.2% of the anti-co area but since they are collimated between the two layers see only 12% of the sky and thus contribute negligibly to the non-vetoed detector area.

The LVSID detectors for IXO/XMS will consist of two arrays of 9 detectors arranged vertically as shown in Figure 7. The two layers are offset by 2mm to cover the gaps between the devices as shown in Figure 8. With a 0.5 mm gap, and a 0.5 mm spacing between the top and bottom surfaces of the two layers, there is no path for charged particles that doesn't intersect one or both devices except at 8 intersection points in the interior of the array. The intersection points between the gaps in the layers give 0.5 x 0.5 mm dead layer columns that open into gaps in the opposing layer. Because the charged particle leaves energy above threshold for even small traversals of the 0.5 mm thick LVSID detector, the maximum opening angle of the intersection is a cross of 36x53 degree views of the sky (x 2 for views out both sides of the stack) or a total view of 1.5 steradians or 12% of the sky. Thus the open area of the 8 intersection points is 0.2% (for a 31.5x31.5 mm detector above the anti-co) but the sky exposure for these intersections is only 12% giving a geometric unvetoed area of 0.02%, which is negligible and predictable on the detector array. The affect of the intersections is actually even lower since only minimum ionizing particles with nearly vertical trajectories deposit energies in the science band (<12 keV) of the XMS. Events with oblique trajectories are vetoed without the aid of the anti-coincidence detector so the actual unvetoed view of the sky is much smaller than 0.02%.

The double layer of LVSID detectors for the IXO/XMS has the additional benefit of being able to distinguish between minimum ionizing particles which deposit energy in the detector array and both layers of the anti-co, from secondary gammas, x-rays, and electrons which will only deposit energy in either the detector array or one layer of the anti-co. This will largely eliminate false-positive vetoes for secondary particles that interact in only one layer of the anti-co.

The readout for the LVSID detector array will use a standard Astro-E2/XRS 18 channel FET box as shown in figure #9. For Astro-E2, one FET channel per FET box was used for the anti-co, 16 for the microcalorimeter array, and 1 unused spare. All 18 FET channels are identical. There were two identical FET boxes per focal plane assembly. For IXO/XMS we will use all 18 FET channels as anti-co channels to read out the 18 channel LVSID array. No changes to the Astro-E2 (and Astro-H) design are necessary. The Astro-E2 FETs operated with low noise, and no radiation damage until the solid neon ran out 22 months after launch and thus have extensive on-orbit heritage. The JFET module is TRL 9.

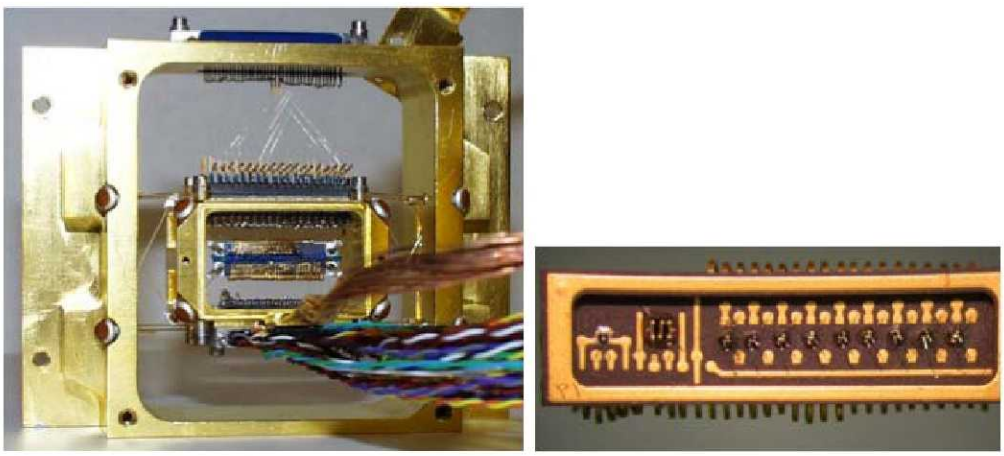

Figure 9. (left) An 18 channel Astro-E2/XRS JFET box and (right) a closeup of 1 (of 2) 9 channel (plus heater and thermometer) JFET packages that are installed in the very center of the JFET box. The JFETs are operated at 130K but thermally isolated with a double Kevlar suspension from the heat sink temperature which was 1.3K on Astro-E2 but would be ~4K on IXO/XMS. Two of these JFET boxes are used on Astro-E2 (and Astro-H/SXS) where only one is needed for the IXO/XMS anti-coincidence detector.

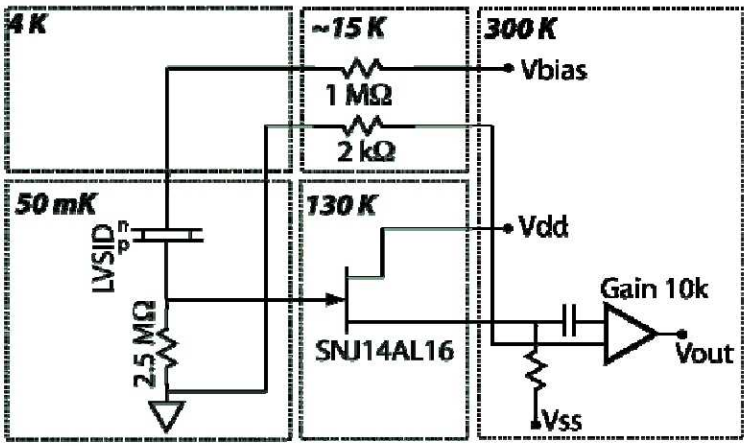

Figure 10. Schematic of the readout of a single LVSID "pixel" showing the bias circuit, cooled JFET transimpedance amplifier, and room temperature preamplifier. This is identical to the readout used on Astro-E2/XRS and Astro-H/SXS using identical subassemblies and electronics boxes.

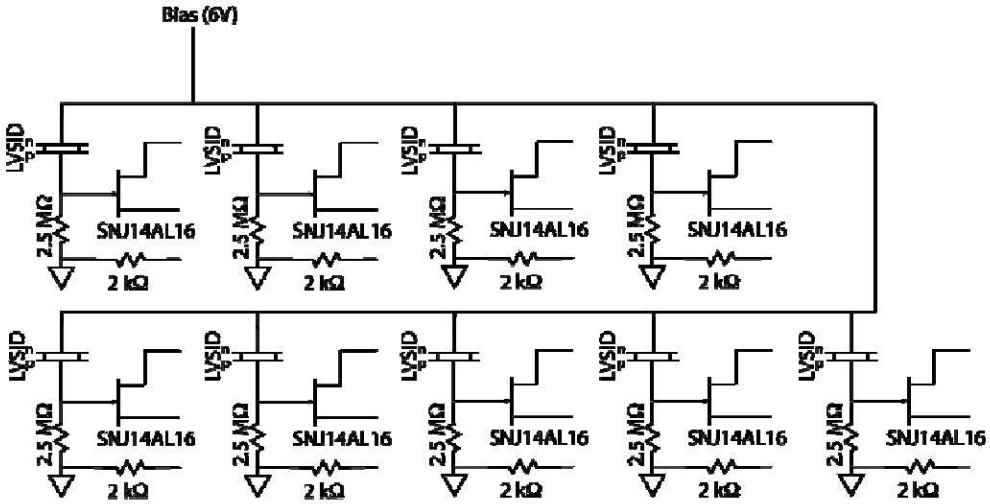

Figure 11. Using an Astro-E2/XRS JFET box, the 18 anti-co pixels are divided into two 9 pixel "sides". Each channel in a side is electrically independent except for a common bias and a common JFET drain. The two "sides" are entirely electrically independent all the way through the room temperature electronics to maintain segmentation. If an entire "side" is lost, the XMS continues to operate with slightly degraded background veto around the edges of the anti-co pixels.

A sketch of the readout circuit for a single XMS anti-co pixel is shown in Figure 10. For IXO/XMS we will use a single readout per channel since the loss of a single LVSID pixel does not seriously impact the operation of the detector, i.e. the two layers allow the anti-co array to degrade gracefully. Since the capacitance of the IXO/XMS LVSID/pixel plus a single readout is almost identical to an Astro-H/SXS LVSID plus two readouts, we expect the time constants of the devices to be the same. Due to the 50% smaller bias resistor, both the SXS and XMS LVSID detectors will be about twice as fast as the Astro-E2/XRS LVSID. The XRS pulse shown in Figure 4 has a risetime of 12 us and a falltime of 260 us. The XMS device will be about 10 us rise and about 130 us fall with a threshold below 20 keV. Every pixel of the LVSID detector has its own independent JFET amplifier and readout chain, however bias and the drain of the JFET are shared in 9 channel groups. Thus each detector layer will have its own 9-channel group of JFETs providing some segmentation against failure. The room temperature amplifiers and JFET control will be identical to the Astro-H design, which itself is almost identical to the Astro-E2 design but implemented in modern class S spaceflight components. A sketch of a 9 channel array "segment" is shown in Figure 11.

4 Summary and Future work

The LVSID anti-coincidence detector, its cryogenic JFET readout, and its room temperature electronics have been operated successfully for almost 5 years on orbit on the Astro-E2 (Suzaku)/XRS instrument. The technology is very simple and the LVSID components, the JFET subassembly, and the room temperature electronics are all TRL 9. The expansion from one device to 18 devices requires no technology development as our ability to array and wirebond individual devices on a 1 cm pitch is well established. The LVSID devices

themselves are trivial to manufacture at any size, and the change from the Astro-E2 and Astro-H 1 cm^2 to 1.3 cm^2 requires no development. In fact, for Astro-E1 the devices were made at wafer scale, i.e. 4" diameter LVSID detectors that were then diced to 1 cm square. The 4" device is also completely operational. The Astro-E2 devices were changed to lithographic definition only to eliminate any breakdown tendency at the edges. An IXO LVSID anti-coincidence array requires no development work and could have substantial re-use of Astro-E2/XRS and Astro-H/SXS components.

The main difference between the primary, TES based anti-co technology and the LVSID backup technology is the mixing of technologies in the focal plane. The primary technology uses the same SQUID multiplexors and room temperature electronics as the x-ray focal plane detectors. An LVSID anti-co would require the addition of JFET preamplifiers and its own room temperature electronics, adding some complexity to the focal plane design and an additional electronics box at room temperature. In either case, the anti-co pulse analysis would be handled in the same way as the focal plane array, and by the same electronics.

There are several ways to reduce the added complexity and increase the performance of an LVSID anti-co for the IXO focal plane with a small development effort. JFET transimpedance amplifiers were chosen to readout the LVSID detector for Astro-E2 and Astro-H not because they were well matched to the LVSID but because they were already implemented for the microcalorimeter array and thus required only the addition of one identical readout channel. However, other techniques could be employed that require less thermal staging and that would reduce the effect of readout capacitance and thus increase the speed of the device. The easiest would be to switch from JFETs at 130K to GaAsFETs which can operate at 4 K. This eliminates the need for thermal control and thermal isolation of the JFET assemblies, vastly simplifying the JFET module. GaAsFETs have higher 1/f noise which is why they are not used for silicon microcalorimeter readout, but they are acceptable for the LVSID detectors. In addition, adding a feedback line to the JFET would allow the use of a charge preamplifier rather than a voltage preamplier at room temperature significantly speeding up the fall time of the detector. In this scheme, the fall and rise time of the detector can be optimized to be approximately symmetric, increasing the device speed to about 10 us fall time. Finally, a SQUID amplifier can be used to read-out an LVSID detector although it requires a very large input inductance to match the impedance of the LVSID. However, the advantage of a SQUID readout is that it could be implemented at 50 mK and eliminate the need to employ JFETs at all.